

Surrogate based wind farm layout optimization using manifold mapping

Kaja Kamaludeen, S.M.; van Zuijlen, A.H.; Bijl, Hester

DOI

[10.1088/1742-6596/753/9/092005](https://doi.org/10.1088/1742-6596/753/9/092005)

Publication date

2016

Document Version

Final published version

Published in

Journal of Physics: Conference Series

Citation (APA)

Kaja Kamaludeen, S. M., van Zuijlen, A. H., & Bijl, H. (2016). Surrogate based wind farm layout optimization using manifold mapping. *Journal of Physics: Conference Series*, 753(9), Article 092005. <https://doi.org/10.1088/1742-6596/753/9/092005>

Important note

To cite this publication, please use the final published version (if applicable). Please check the document version above.

Copyright

Other than for strictly personal use, it is not permitted to download, forward or distribute the text or part of it, without the consent of the author(s) and/or copyright holder(s), unless the work is under an open content license such as Creative Commons.

Takedown policy

Please contact us and provide details if you believe this document breaches copyrights. We will remove access to the work immediately and investigate your claim.

Surrogate based wind farm layout optimization using manifold mapping

This content has been downloaded from IOPscience. Please scroll down to see the full text.

2016 J. Phys.: Conf. Ser. 753 092005

(<http://iopscience.iop.org/1742-6596/753/9/092005>)

View [the table of contents for this issue](#), or go to the [journal homepage](#) for more

Download details:

IP Address: 131.180.130.242

This content was downloaded on 28/02/2017 at 13:31

Please note that [terms and conditions apply](#).

You may also be interested in:

[Polynomial chaos for the computation of annual energy production in wind farm layout optimization](#)

A S Padrón, A P J Stanley, J J Thomas et al.

[Surrogate models for efficient stability analysis of brake systems](#)

Lyes Nechak, Frédéric Gillot, Sébastien Besset et al.

[Twin surrogates to test for complex synchronisation](#)

M. Thiel, M. C. Romano, J. Kurths et al.

[A surrogate model enables a Bayesian approach to the inverse problem of scatterometry](#)

S Heidenreich, H Gross, M-A Henn et al.

[Influence and measurement of mass ablation in ICF implosions](#)

B Spears, D Hicks, C Velsko et al.

[MF-DFA Analysis of Turbulent Transport Measured by a Multipurpose Probe](#)

M. Lafouti and M. Ghoranneviss

[Erratum: Extended self-similarity of atmospheric boundary layer wind fields in mesoscale regime: Is it real?](#)

V. P. Kiliyanpilakkil and S. Basu

[Global design optimization for an axial-flow tandem pump based on surrogate method](#)

D H Li, Y Zhao and G Y Wang

[BH Masses of Soft X-Ray-Selected AGNs](#)

Linda C. Watson, Smita Mathur and Dirk Grupe

Surrogate based wind farm layout optimization using manifold mapping

Shaafi M Kaja Kamaludeen, Alexander van Zuijlen, Hester Bijl

Faculty of Aerospace Engineering, Delft University of Technology, 2629 HS Delft, The Netherlands

E-mail: s.m.kajakamaludeen@tudelft.nl

Abstract. High computational cost associated with the high fidelity wake models such as RANS or LES serves as a primary bottleneck to perform a direct high fidelity wind farm layout optimization (WFLO) using accurate CFD based wake models. Therefore, a surrogate based multi-fidelity WFLO methodology (SWFLO) is proposed. The surrogate model is built using an SBO method referred as manifold mapping (MM). As a verification, optimization of spacing between two staggered wind turbines was performed using the proposed surrogate based methodology and the performance was compared with that of direct optimization using high fidelity model. Significant reduction in computational cost was achieved using MM : a maximum computational cost reduction of 65%, while arriving at the same optima as that of direct high fidelity optimization. The similarity between the response of models, the number of mapping points and its position, highly influences the computational efficiency of the proposed method. As a proof of concept, realistic WFLO of a small 7-turbine wind farm is performed using the proposed surrogate based methodology. Two variants of Jensen wake model with different decay coefficients were used as the fine and coarse model. The proposed SWFLO method arrived at the same optima as that of the fine model with very less number of fine model simulations.

1. Introduction

Acute hunger towards cleaner energy drives the fast growing offshore wind energy to build larger wind farms with mammoth wind turbines. Due to the high initial investment cost, these large wind farms need to be highly efficient. Even a marginal increase in efficiency will significantly increase the profit (i.e. in the scale of millions of Euros). Wind farm layout optimization (WFLO) is one of the crucial steps in the design of these wind farms and is performed to optimize the power production directly or indirectly through certain objective functions such as annual energy production (AEP), cost of energy (COE), Leverized Cost Of Energy (LCOE) etc. During the optimization process, different possible layouts are generated, and the expected power production (and structural loads in case of multi-objective WFLO) of these layouts are estimated using wake models. The power production is heavily influenced by some dominant flow features such as turbine-wake interaction and turbine-ABL (atmospheric boundary layer) interaction. The wake model which is used to model the flow field inside the wind farm should capture these dominant physical factors for a reliable power prediction.

WFLO is a highly complex constrained non-linear optimization problem and an area of active research, which involves finding optimal turbine locations inside the wind farm area such



that the objective function(s) is(are) optimized. Since conventional gradient based optimization methods have a high probability of converging to a poor local optimum, heuristic methods such as genetic algorithm (GA), particle swarm technique (PSO) are most suited for WFLO [1]. Most of such WFLO methods are population-based methods which involves analyzing the evolution of multiple populations (i.e. wind farm layouts). For every evolution of the individual population, the wake model has to be used to estimate the extracted power and this ample use limits the computational affordability of the wake models. Hence, the prevalent wind farm wake models such as Jensen, Ainsle, Larson etc [2] are computationally cheap empirical models. These wake models are generally of low accuracy since they are based on superimposition of steady state approximations or solutions of the individual turbine in a simplified flow condition or assumptions.

The wake models should include the effects of dominant flow physics notably the turbine-wake interactions and atmospheric boundary layer (ABL) interaction in order to accurately estimate the wake loss, wake recovery and the fatigue loads. To capture these flow features, the wind farm should be modeled using high-fidelity computational models such as LES, RANS. Due to the enormous computational cost associated with it, using those models directly as wake models during WFLO is not feasible. Schmidt and Stoevesandt [3] proposed a new CFD based method, where the results of RANS simulations are superimposed to build the wind farm flow field. But the interaction of ABL with large wind farm cannot be captured with this approach since it requires simulation of the whole wind farm. To alleviate this issue, surrogate-based optimization(SBO) methods can be a good feasible alternative which can reduce the computational cost to a huge extent.

The present scenario of simulation based objective functions with high computationally cost (expensive high fidelity simulations) is encountered more commonly in the field of electromagnetics and circuit design. In such cases, SBO methods are used to solve the optimization problem efficiently using very few high-fidelity simulations [4, 5]. In SBO, the computationally intensive design variable search (search in design space) is performed using surrogate models which are computationally cheap approximation of expensive high fidelity model. During this iterative procedure, the high fidelity model is evaluated at carefully selected points obtained using the surrogate. After every iteration, the surrogate is updated with the newly available high fidelity data and the accuracy of the surrogate is improved and thus, near optimal design can be obtained efficiently. The surrogate can be an analytical surrogate i.e. surrogate built based on analytical functions such RBF or kriging using the design of experiment (DOE) or a physical surrogate i.e. a computationally cheap physical model with simplified assumptions. SBO based optimization methods have also been used by few researchers to accelerate the optimization of aerofoil shapes [6,7]. In such studies, a computationally expensive RANS model with a fine grid was used as high fidelity model, and coarse grid [6] or a partially converged solution [7] was employed as a low fidelity model. Some of the popular SBO methods currently being used are space mapping (SM), manifold mapping (MM), shape preserving response prediction (SPRP) and adaptive response correction (ARC).

Mehmani et. al. [8] proposed a surrogate based methodology for WFLO problem coupled with particle swarm optimization technique (PSO). They used a kriging based analytical surrogate, built using an SBO method called adaptive model refinement (AMR). One of the main pitfalls of SBO methods is that the surrogate model (especially the analytical ones like kriging) may not be valid in the whole design space, thereby leading to sub-optimal or infeasible solutions. Mehmani et. al. circumvented this bottleneck by infusing more number of in-fill points (high fidelity runs) to improve the local as well as the global accuracy of the surrogate. This again increases the computational load since it still relies on the heavy usage of high fidelity model.

The number of high fidelity runs can be reduced by the using an appropriate physical sur-

rogate rather than analytical ones (multi-fidelity approach). By choosing a physical surrogate which can capture some dominant physical phenomena, the efficiency of the SBO methods can be improved. For instance, existing wake models which can model the wake loss up to a reasonable accuracy can be used as low fidelity model and the surrogate built on top of it is expected to be more efficient than the analytical surrogate. In this present study, one of the most widely used engineering wind turbine wake model, Jensen wake model is used as a low fidelity model, and the surrogate model is built using manifold mapping (MM). The proposed method needs one high fidelity simulation per iteration to update surrogate, compared to the set of infill points in case of AMR. The proposed method can be implemented within any existing WFLO framework without any major modifications.

2. Methodology

In 1994, Bandler[9] conceived a multi-fidelity SBO method referred as space mapping (SM), to avoid the direct optimization of an expensive fine model. Space mapping employs a computationally cheap but less accurate low fidelity model (also referred as the coarse model) and an expensive primary high fidelity model (or fine model). Space mapping establishes a parameter mapping (mapping between the design parameters) between these two models such that the response of two models is same. In space mapping technique, the surrogate is the mapping augmented low fidelity model. Thus under perfect mapping, optimization of expensive high-fidelity model is equivalent to optimizing the computationally cheap, mapping augmented low fidelity model. Hence there is a huge reduction in computational cost. Since then, several modified versions of space mapping have been proposed under SBO methods such as aggressive space mapping, implicit space mapping, output space mapping, etc [10]. Echeiverria [11] proposed a version of output space mapping referred to as manifold mapping (MM). Unlike other space mapping methods, he supported the method with a sound mathematical proof of convergence using defect correction theory.

In MM technique, the mapping is established between the response (i.e. output) of the fine model and the coarse model rather than the design parameters. Let $f(\mathbf{x})$ and $c(\mathbf{x})$ be the response of the fine model and the coarse model. The surrogate model is given by $S_k(\mathbf{x})$. The pseudo-code of original manifold mapping (OMM) used in the present study is shown in Algorithm 1. It can be seen that the original optimization of the fine mode $\mathbf{x}^* = \operatorname{argmin} \|f(\mathbf{x}) - y\|$ is replaced by an iterative optimization of the surrogate $\mathbf{x}_k = \operatorname{argmin} \|S_k(\mathbf{x}) - y\|$. After every MM iteration, the fine model is re-evaluated for the latest obtained optimal design and the surrogate model is updated using the new high fidelity data. Since the high fidelity model is used to correct the response of the coarse model rather than using it for the optimization itself, the computational load is reduced drastically.

The success of manifold mapping is dependent on how well the mapping corrects the misalignment between the response of the coarse model and fine model. The mapping between the models is performed using affine mapping and is given by:

$$S_{k+1}(\circ) = f(\mathbf{x}_{k+1}) + \mathbf{S}_{k+1}(\circ - c(\mathbf{x}_{k+1})), \quad (1)$$

where \mathbf{S} , is the mapping matrix. It is given by:

$$\mathbf{S}_{k+1} = \Delta F \Delta C^\dagger. \quad (2)$$

ΔF and ΔC are the approximated Jacobians of coarse and fine models respectively. ΔC^\dagger refers to pseudo inverse obtained using singular value decomposition. The affine mapping can be explained using Figure 1. Let the blue solid line represent response of the coarse model ($c(\mathbf{x})$) while the red solid line represent response of the fine model ($f(\mathbf{x})$). The mapping should translate

```

 $\mathbf{x}_0 = \mathbf{x}_c^* = \operatorname{argmin} \|c(\mathbf{x}) - y\|;$ 
 $S_0(\circ) = f(\mathbf{x}_0) + (\circ - c(\mathbf{x}_0));$ 
for  $k=0,1,2\dots$  do
     $\mathbf{x}_{k+1} = \operatorname{argmin} \|S_k(c(\mathbf{x})) - y\|$ 
    break if(converged)
     $\Delta F = [f(\mathbf{x}_{k+1}) - f(\mathbf{x}_k), \dots, f(\mathbf{x}_{k+1}) - f(\mathbf{x}_{\max(k+1-n,0)})]$ 
     $\Delta C = [c(\mathbf{x}_{k+1}) - c(\mathbf{x}_k), \dots, c(\mathbf{x}_{k+1}) - c(\mathbf{x}_{\max(k+1-n,0)})]$ 
     $\Delta C = U_c \Sigma_c V_c^T$ 
     $\Delta C^\dagger = V_c \Sigma_c^\dagger U_c^T$ 
     $\mathbf{S}_{k+1} = \Delta F \Delta C^\dagger;$ 
     $S_{k+1}(\circ) = f(\mathbf{x}_{k+1}) + \mathbf{S}_{k+1}(\circ - c(\mathbf{x}_{k+1}));$ 
end
    
```

Algorithm 1: Original Manifold mapping (OMM)

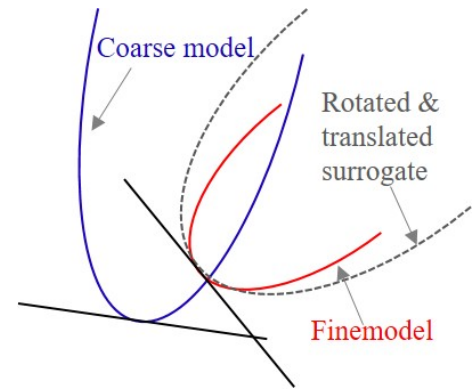


Figure 1: Manifold mapping - pictorial illustration

and rotate the response of the coarse model such that the extremum (minimum in this case) of the surrogate (i.e. mapping augmented coarse model) is same as that of the fine model. The affine mapping maps both the value as well as the approximated gradient of the available fine model response. The mapping matrix is initialized with unity matrix $S_0(\mathbf{x})$ and is updated with the fine model response after every MM iteration. As this iterative procedure continues, the approximated Jacobians becomes more and more accurate, and as per MM theory, the perfect mapping occurs at the local minimum of the fine model. In other words, the manifold mapping converges to the local minimum of the fine model. Detailed derivation of the algorithm and its convergence proof can be found in the thesis of Echevierria [11].

One of the criteria to use MM is that the number of responses from the models (both fine and coarse) should be more than that of the design variables. However, in most WFLO, the number of design variables is greater than the number of objective function, which is usually a single variable like AEP or COE. Hence, to satisfy the criteria, additional information or quantities which will influence the objective function are included in the response of the models. Few recommended quantities are velocities measured at prescribed locations (also referred as mapping points in this paper), power generated by individual turbines, turbine loads in case of multidisciplinary optimization, etc. Since the power output of the wind turbine is usually interpolated from the power chart based on the velocity measured at the centre of the actuator disc (i.e. turbine hub), these points (hub velocities) are always included in the mapping points. The modified algorithm of WFLO using the present SBO methodology is shown in Figure 2. The proposed methodology is a black box model in which any existing wake models and optimization strategy can be used.

3. Verification

To verify the proposed methodology, an academic optimization of a small wind farm with two staggered wind turbines is performed. The optimization is performed to find the optimal spacing between two turbines such that the cost of energy is minimal. The total cost is a function of spacing between the turbines. Since the downstream turbines will always be inside the wake of upstream one, the main flow phenomena that determines the optimal spacing is the wake recovery behind the upstream turbine. By choosing a fine model which can capture this wake recovery accurately (a viscous solver) and a coarse model which cannot capture the wake recovery (inviscid solver), the robustness of the proposed methodology can be studied. The SBO

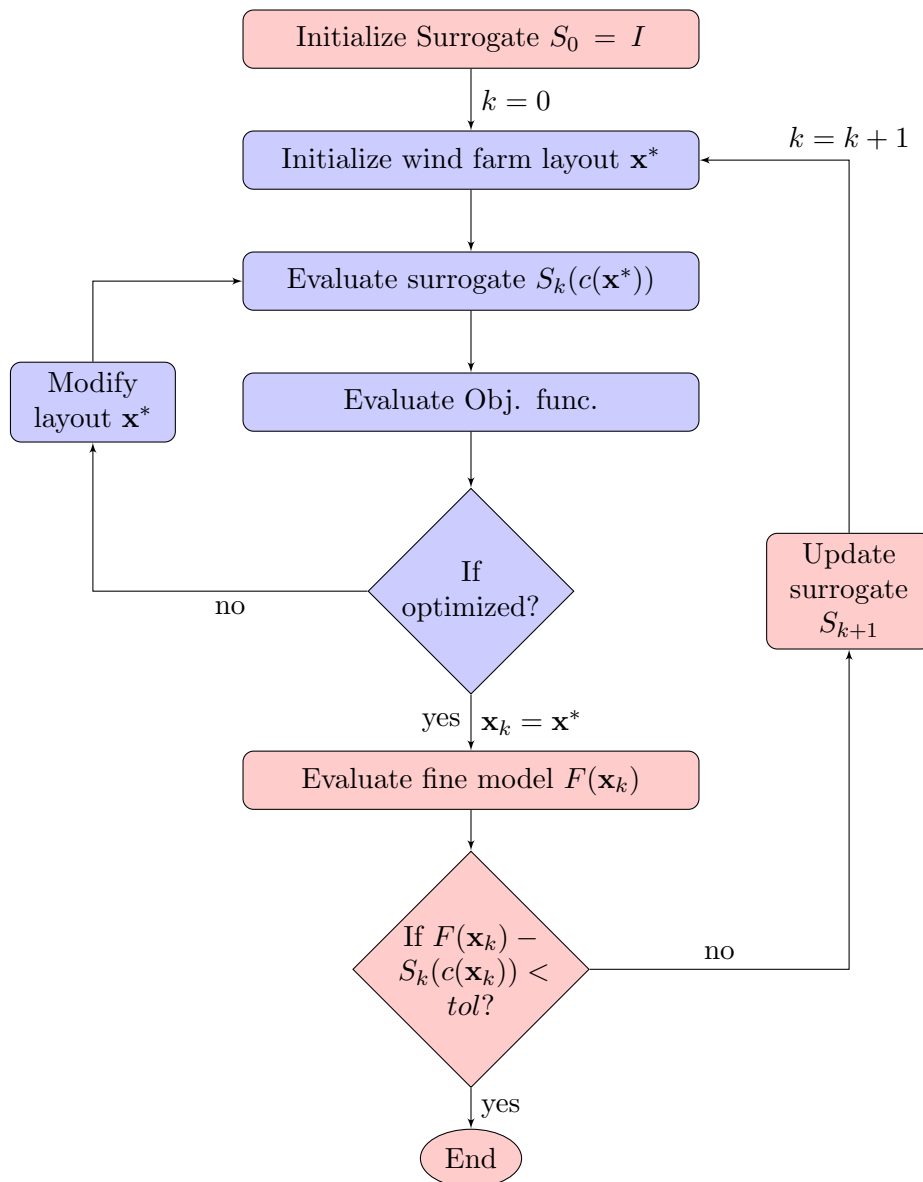


Figure 2: SBO based wind farm layout optimization.

based optimization should arrive at the same optimal spacing as that of direct optimization using viscous fine model.

The flow is assumed to be two-dimensional and laminar ($Re = 100$). The wind turbines are modeled as two-dimensional actuator disc with uniform loading across the disc. Single wind sector is considered for this validation study i.e. wind flowing from only one direction (270°). The actuator disc is applied with a constant thrust coefficient ($C_t = 1$) and the power is assumed to be a cubic function of velocity measured at the center of actuator disc ($P = U_d^3$, where U_d is the axial velocity measured at the center of the disc). A finite difference method based viscous solver which can capture the viscous wake recovery accurately is used as the fine model. The convergence of the manifold mapping is highly dependent on the choice of coarse model. As per MM theory, convergence can be improved by choosing similar models (i.e. fine and coarse model). To check the coarse model dependency of the proposed method, two different

low fidelity models are considered for this validation study. One is an inviscid vortex particle model (VPM) based free wake model (inviscid VPM), and the other is a viscous VPM solver with diffusion modeled through core spreading technique. The coarse models are intentionally made less accurate by using less number of vortex particles.

The centreline velocity of the wake of a single actuator disc obtained from different models is shown in Figure 3. It can be seen that the inviscid VPM cannot capture the wake recovery, while the other coarse model (viscous VPM) can capture the wake recovery but with less accuracy. The objective of this feasibility study is to check whether the surrogate built using MM can pass the flow physics i.e. viscous wake recovery from the high fidelity model to the low fidelity model accurately. The intention of the proposed surrogate based WFLO is to include the effect of ABL interaction during WFLO with minimal computational cost. The wake recovery caused due to the viscous diffusion in the present case can be compared with the wake recovery influenced by the ABL interaction in case of large wind farms. Hence, the choices made in this validation study reflects the similar scenario encountered in real life WFLO.

As mentioned in the previous section, the number of responses of the models (m) (i.e. fine, coarse and surrogate) should be higher than that of the number of design variables (n). In present study, the only design variable ($n = 1$) is the non-dimensionalized distance between the two turbines (S/D , where D is the diameter of the turbine). Hence the size of response vector (m) should be greater than one. The least number of responses that can be mapped are the velocities at the center of each actuator disc ($m = 2$), since it will be needed to calculate the power. Since the size of the mapping matrix \mathbf{S} is equal to the length of response vector (m), the surrogate can map the value and gradient at maximum two latest obtained spacings. By increasing the number of responses (m), the size of mapping matrix is also increased so that surrogate can retain more number of fine model data. This will improve the global accuracy of the surrogate. To study the influence of number of responses (m), the validation study is performed with four different sets of mapping points as shown in Figure 4, where TD_m refers to training data with m response. The base case corresponds to $m = 2$ and three other test case corresponds to $m = 3, 6$ & 45 . The optimization is performed using one of the Matlab's minimization routine, *fmincon*. Direct optimization of the fine model (direct high-fidelity optimization) using the same minimization routine (*fmincon*) is also performed to verify the optimal spacing obtained from MM based optimization and to compare its performance.

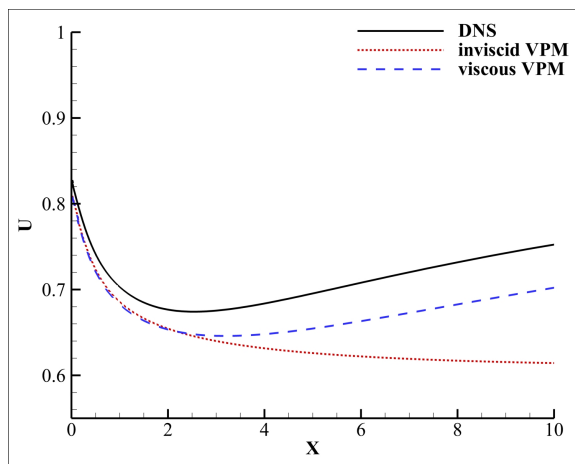


Figure 3: Centreline velocity behind an actuator disc.

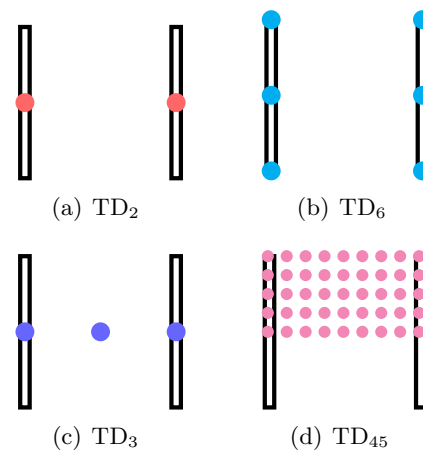


Figure 4: Mapping points selections.

Table 1: Results of SWFLO.

	Direct	Inviscid VPM-SWFLO				Viscous VPM-SWFLO			
case		TD ₂	TD ₆	TD ₃	TD ₄₅	TD ₂	TD ₆	TD ₃	TD ₄₅
Optimal spacing (x/D)	10	10	10	10	10	10	10	10	10
High fidelity model runs	11	8	7	5	5	7	5	6	4
Low fidelity model runs	NA	75	65	39	38	63	42	54	30

Table 1 shows the performance and the results of MM based optimization along with that of direct optimization using fine model (high fidelity model). It can be seen that MM based optimization arrives at the same optimal spacing as that of direct optimization for all the cases considered. Increasing the number of mapping points accelerates the convergence of MM, thereby reducing the number of fine model runs or MM iterations. Looking at the performance of TD₆ and TD₃, the location of mapping points also influences the convergence. It can be seen that for inviscid VPM as the coarse model, the inclusion of just one mapping point in the wake region accelerates the convergence. However, the influence is quite the opposite for the case with viscous VPM as coarse model. Further studies will be required to derive a solid conclusion regarding the location of mapping points. Maximum computational reduction of 65 % is observed for TD₄₅ with viscous VPM as the coarse model. The observed computational cost reduction is for a simple academic test case with one degree of freedom (design variable). But the real advantage of the MM can be observed in problems with more degrees of freedom and in such cases the computational advantage will be tremendous.

Let us examine how the affine transformation maps the response of the fine and coarse model. To study this, the surrogate updated during every MM iteration of case: TD₂ with inviscid VPM as coarse model, is used to model the wake for different turbine spacings separately. Figure 5 shows one of the responses of the evolving surrogate generated during different MM iterations (grey solid lines). The response shown in Figure 5 corresponds to the axial velocity measured at the center of the downstream turbine (U_{d2}) with respect to turbine spacing. Figure 5a corresponds to the response of surrogate updated during the first MM iteration and Figure 5b - d corresponds to the response of surrogate updated during iterations 2, 5 and 6. The response of the coarse model (blue solid lines) and the fine model (red solid lines) is also shown for comparison. During the first MM iteration, the surrogate will have information of only one fine model response. Hence the surrogate can only translate the coarse model response, and the perfect match was observed at the initial guess (Figure 5a). During the subsequent iterations, the response of coarse model was rotated such that both the value of the velocity as well its gradient are mapped with the latest obtained fine model data. Towards the final iterations (MM iteration 6), a perfect mapping was observed close to the optimal spacing of $S/D = 10$. Since $m = 2$ (no. of response), the surrogate can map the values and gradient of latest two fine model data. Hence, the surrogate response deviates from the fine model response for small inter turbine spacing. For all other cases (i.e. TD₆, TD₃ and TD₄₅) with large number of responses, a better mapping was observed.

Since it is difficult to deduce a methodology to select the mapping points based on the present study, it is advised to choose few points along the actuator disc or turbine and in the

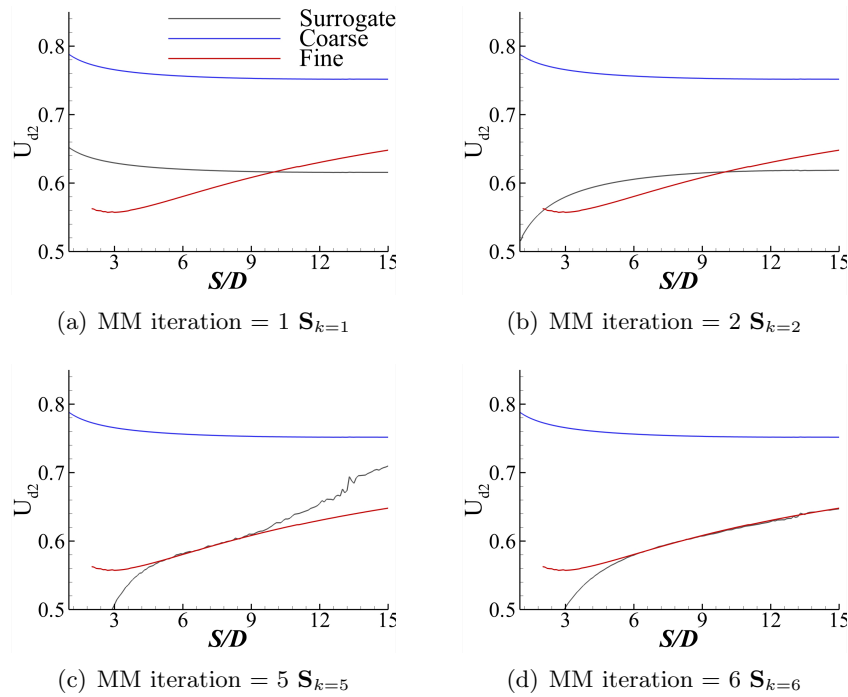


Figure 5: Velocity measured at centre of downstream turbine (U_{d2}) by surrogate

Table 2: Wind sectors data

Wind angle (degrees)	Wind speed (m/s)	Wind frequency (%)
30	6.92	13.4
120	7.46	24.4
210	8.27	27.5
300	8.53	34.8

wake region similar to TD₄₅. Care should be taken to prevent repetition of mapping points with similar behavior. The mapping points should be unique to prevent singularity of mapping matrix. For instance, in case TD₆, the top and bottom points on the disc will behave similar due to symmetry. This repetition of similar points will reduce the rank of the approximated Jacobian and may lead to singular mapping matrix if sufficient care is not taken.

4. Case study: realistic WFLO using Genetic Approach

In previous section, the proposed surrogate-based optimization methodology is validated for a simple test case with one degree of freedom i.e. one design variable ($n = 1$). However, in case of realistic WFLO, the number of design variables will be twice the number of turbines and SBO methods are meant to tackle such computationally intensive optimization problems. As a proof of concept and to demonstrate the proposed method, surrogate based WFLO of a realistic wind farm is performed.

4.1. Details of wind farm

The proposed method is used to design a 7-turbine wind farm inside a square area of size $5D \times 5D$, where D is the diameter of wind turbine. The numerical wind turbine considered for the present study is NREL's 5MW reference wind turbine with a rotor diameter of 126 m and hub height of 90 m. More details on the wind turbine can be found in [12]. A synthetic wind rose of four wind sectors is considered (Table 2). Even though it is advisable to use large number of wind sectors for an accurate WFLO, only four sectors are considered in the present case study to keep the computational time minimal. Since the wind farm area is very small, the turbines have to be densely packed. This will result in pronounced turbine-wake interactions leading to considerable wake loss. Hence, the accurate capturing of wake recovery is required to design an aerodynamically efficient wind farm. The number of wind turbines is assumed to be constant and hence the installation cost, which is a function of number of turbines, will also remain the same. Therefore, maximizing the efficiency will be equivalent to minimizing the COE [13].

4.2. Optimization methodology

Unlike the validation study, the realistic WFLO is much more complex with multiple local maxima. For this reason, heuristics based optimization techniques such as Genetic Algorithm (GA), Particle swarm technique (PSO) are more commonly used. In the present case study, a genetic algorithm similar to the one proposed by Mosetti et. al. [13] is used to perform optimization. For a detailed description of GA, the readers can refer to [13]. Mosetti et. al. [13] divided the entire wind farm area into a certain number of cells and the turbines are allowed to be placed at the center of these cells. This cell-based approach makes the solution space discrete, and the GA cannot explore the intermediate location other than the cell centers. To overcome this, in present study, the turbines are allowed to take any random position within the wind farm area. In other words, the design variables i.e. the coordinates of the turbines are treated as continuous variables and the turbines are allowed to take any random location as long as it satisfies two constraints similar to constraints used by Perez et. al. [14]. One constraint is that the coordinates of the turbines should fall within the wind farm area, and other is a proximity constraint such that minimum distance between any two turbines of a layout is always greater than $2D$.

One of the objectives of this case study is to prove that the MM based WFLO converges to the same optimum layout as that of conventional WFLO using high fidelity wake model but with minimal usage of high fidelity wake model. In this proposed methodology, the GA based optimization of wind farm layout will be performed using the surrogate wake model during every MM iteration. If the GA is allowed to generate new random layouts (initial parent individuals) during every MM iteration, it will be difficult to perform the above-mentioned verification. Hence, the GA is initialized with pre-generated layouts (fixed initial population) during every MM iteration. The GA is initialized with a population of 100 individuals, which are allowed to evolve for 50 iterations. Mosetti et. al. [13] used cross over rate of $0.6 < P_c < 0.9$ and mutation rate $0.01 < P_m < 0.1$ for a good evolution of initial population. In the present study, 20 % of the best performing initial population are allowed to mutate with a mutation rate P_m of 0.02. Unlike Mosetti et. al. [13], higher cross over rate of $P_c = 1.0$ is used in present study. The crossover and mutation operations performed are similar to that of [13] except for one variation. Instead of binary numbers, the coordinates are exchanged during the crossover between two parents. With the above-mentioned settings, the GA always converged to the best layout among the initial pre-generated layouts within 20 iterations.

4.3. Manifold mapping settings

The mapping points considered in this case study is similar to that of TD₄₅ of the validation study. 21 mapping points are chosen for each wind turbine. The location of mapping points is dependent on the orientation of the wind turbine (i.e. wind direction). Figure 6 shows the distribution of mapping points for a wind turbine. The response vector of the models consists of power generated by each wind turbine, followed by the velocity measured at the mapping points and is repeated for all the wind sectors. For the present case of 7 wind turbines and 4 wind sectors, the length of response vector is 616, which is higher than that of the design variables.

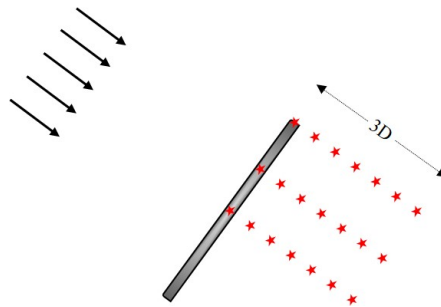


Figure 6: Distribution of mapping points

4.4. Wake model

Two variants of Jensen wake models with different decay coefficient k is used as the fine and coarse model. For the coarse model, decay coefficient of $k = 0.04$ is used and for the high model a very high decay coefficient of $k = 0.12$ is used. The above-mentioned decay coefficient is used only to calculate the wake deficit. For the calculation of wake radius, decay coefficient of $k = 0.04$ is used for both the models. The initial pre-generated individuals or layouts used in present study is shown in Figure 7 (red marker circles). The conventional GA based direct optimization using fine and coarse models (done separately) arrives at different optimal layouts and is pointed out in Figure 7 using blue and black bold markers.

4.5. Discussions

Following the direct optimization, the study was repeated using the proposed MM based approach. The MM based WFLO arrived at the same optimal layouts as that of the fine model in 2 MM iterations. The norm of the various error observed optimization process is shown in Table 3. During the first MM iteration, the optimal layout was same as that of the coarse model. In other words, mere translation of the coarse model was not sufficient. However, in the next iteration, the surrogate was able to map the response of fine model successfully ($S_k(c(\mathbf{x})) - F(\mathbf{x}) = 0$). Using the updated surrogate, the present method arrived at same optimal layout as that of the fine model ($\Delta X = 0$). The optimization was continued till the error in the response of surrogate converges below the tolerance level. Although, in practice, the optimization can be stopped with the convergence of ΔX and $S_k(c(\mathbf{x})) - F(\mathbf{x})$. The superior convergence of MM observed in this case study is attributed to the close similarity between the fine and coarse model.

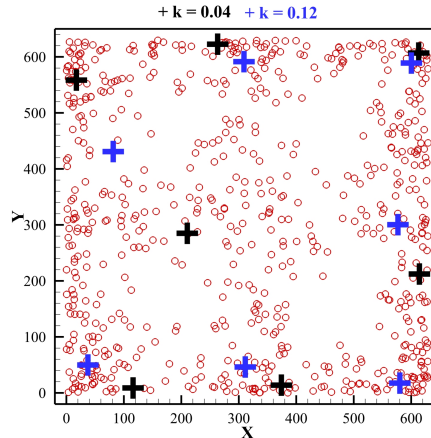


Figure 7: Collocated random layouts with optimal turbine locations

Table 3: Case study: Error norms observed during MM based WFLO

MM iter	ΔX	$S_k(c(\mathbf{x})) - F(\mathbf{x})$	$S_k(c(\mathbf{x})) - S_{k-1}(c(\mathbf{x}))$
1	0	0	1.6984
2	985.31	1.3091	0
3	0	0	1.3091
4	0	0	0

5. Conclusions and recommendations

Surrogate-based WFLO (SWFLO) can be used to perform high-fidelity wind farm layout optimization. It has been shown that the proposed SWFLO converges to the optima of the fine model in both simplified validation study and as well as in more realistic case study. One of the recommendations for performing WFLO is that the optimization strategy should be a combination of both heuristic and gradient-based search. The heuristic approach which searches the design space for a near-optimal solution (global search), followed by a gradient-based search in the vicinity of near-optimal solutions (local search) will lead to an improved design. In such cases, multiple local optima will be encountered during the global search, and the ability of proposed method to circumvent these local optima is not yet studied. A more detailed study will be performed in near future to address this issue.

Recent studies have shown that with advanced SBO methods such as shape preserving response prediction (SPRP) and adaptive response correction (ARC), better performance can be achieved. A comparative study of few such methods will yield a better performing SWFLO.

6. References

- [1] Gonzalez J S, Payn M B, Santos J M and Gonzalez-Longatt F A 2014 *Renewable and Sustainable Energy Reviews* **30** 133-44
- [2] Gocmen T, Laan P, Rethore P, Diaz A P, Larsen G C and Soren Ott 2016 *Renewable and Sustainable Energy Reviews* **60** 752-69
- [3] Schmidt J and Stoevesandt B 2015 *EWEA - Europe's Premier Wind Energy Event*
- [4] Koziel S, Echeverria D and Leifsson L 2011 *Computational Optimization, Methods and Algorithms*, chapter 3 pp 33-59
- [5] Koziel S and Leifsson L 2013 *Surrogate-Based Modeling and Optimization : Applications in Engineering*
- [6] Koziel S and Leifsson L 2013 *AIAA JOURNAL* **51**(1) 94-106
- [7] Forrester A I, Bressloff N W and Keane A J 2006 *Proc. R. Soc. A* **462** 2177-204

- [8] Mehmani A, Tong W, Chowdhury S and Messac A 2015 *World Congress on Structural and Multidisciplinary Optimization*
- [9] Bandler J W, Biernacki R M, Chen S H, Grobelny P A and Hemmers R H 1994 *IEEE Trans. Microwave Theory Tech.* **42**(12) 2536-44
- [10] Bandler J W, Cheng Q S, Dakroury S A, Mohamed A S, Bakr M H, Madsen K and Sondergaard J 2004 *IEEE Trans. Microwave Theory Tech.* **52**(1) 337-61
- [11] Echeverra D 2007 *PhD Thesis*. University of Amsterdam.
- [12] Jonkman J, Butterfield S, Musial W and Scott G 2009 *National Renewable Energy Laboratory, Golden, CO, Technical Report*
- [13] Mosetti G, Poloni C and Diviacco B 1994 *Journal of Wind Engineering and Industrial Aerodynamics* **51**(1) 105-16
- [14] Perez B, Minguez R and Guanche R 2013 *Renewable Energy* **53** , 389-99